



HAL
open science

Combined invariants to similarity transformation and to blur using orthogonal Zernike moments.

Chen Beijing, Huazhong Shu, Hui Zhang, Gouenou Coatrieux, Limin Luo,
Jean-Louis Coatrieux

► To cite this version:

Chen Beijing, Huazhong Shu, Hui Zhang, Gouenou Coatrieux, Limin Luo, et al.. Combined invariants to similarity transformation and to blur using orthogonal Zernike moments.. IEEE Transactions on Image Processing, 2011, 20 (2), pp.345-60. 10.1109/TIP.2010.2062195 . inserm-00522932

HAL Id: inserm-00522932

<https://inserm.hal.science/inserm-00522932>

Submitted on 3 Oct 2010

HAL is a multi-disciplinary open access archive for the deposit and dissemination of scientific research documents, whether they are published or not. The documents may come from teaching and research institutions in France or abroad, or from public or private research centers.

L'archive ouverte pluridisciplinaire **HAL**, est destinée au dépôt et à la diffusion de documents scientifiques de niveau recherche, publiés ou non, émanant des établissements d'enseignement et de recherche français ou étrangers, des laboratoires publics ou privés.

Combined invariants to similarity transformation and to blur using orthogonal Zernike moments

Chen Beijing^{1,2}, Huazhong Shu^{1,2*}, Hui Zhang^{1,2}, Gouenou Coatrieux³, Limin Luo^{1,2*}, Jean-Louis Coatrieux^{1,4*}

¹ CRIBS, Centre de Recherche en Information Biomédicale sino-français INSERM : LABORATOIRE INTERNATIONAL ASSOCIÉ, Université de Rennes I, SouthEast University, Rennes,FR

² LIST, Laboratory of Image Science and Technology SouthEast University, Si Pai Lou 2, Nanjing, 210096,CN

³ ITI, Département Image et Traitement Information Institut Télécom, Télécom Bretagne, Université européenne de Bretagne, Technopôle Brest-Iroise CS 83818 29238 BREST CEDEX 3,FR

⁴ LTSI, Laboratoire Traitement du Signal et de l'Image INSERM : U642, Université de Rennes I, Campus de Beaulieu, 263 Avenue du Général Leclerc - CS 74205 - 35042 Rennes Cedex,FR

* Correspondence should be addressed to: Huazhong Shu <shu.list@seu.edu.cn >

* Correspondence should be addressed to: Limin Luo <luo.list@seu.edu.cn >

* Correspondence should be addressed to: Jean-Louis Coatrieux <Jean-Louis.coatrieux@univ-rennes1.fr >

Abstract

The derivation of moment invariants has been extensively investigated in the past decades. In this paper, we construct a set of invariants derived from Zernike moments which is simultaneously invariant to similarity transformation and to convolution with circularly symmetric point spread function (PSF). Two main contributions are provided: the theoretical framework for deriving the Zernike moments of a blurred image and the way to construct the combined geometric-blur invariants. The performance of the proposed descriptors is evaluated with various PSFs and similarity transformations. The comparison of the proposed method with the existing ones is also provided in terms of pattern recognition accuracy, template matching and robustness to noise. Experimental results show that the proposed descriptors perform on the overall better.

Author Keywords Zernike moments ; circularly symmetric blur ; combined invariants ; pattern recognition ; template matching.

INTRODUCTION

Recognition of objects whatever their position, size and orientation is an important concern. In the past decades, many techniques including moment invariants [1]–[5], Fourier descriptors [6] and point set invariants [7]–[10] have been reported in the literature. Among them, moment invariants have been extensively used for image description in object recognition [11], [12], image classification [13] and scene matching [14]. However, much less attention has been paid to invariants with respect to changes of the image intensity function (known as radiometric invariants) as to joint radiometric-geometric invariants.

Since real sensing systems are usually imperfect and environmental conditions are changing during the acquisition, the observed images often provide a degraded version of the true scene. Image blurring is an important class of degradations we have to face in practice due to the camera defocus, atmospheric turbulence, vibrations, and by sensor or scene motion [15]. Blurring can be usually described by a convolution of an unknown original image with a space invariant point spread function (PSF). A conventional way to carry out blur object recognition is first to deblur the image, and then to apply the recognition methods [16]–[21]. Unfortunately, the blind image deconvolution is an ill-posed problem. Moreover, the deconvolution process may introduce new artifacts to the image. To avoid these disadvantages, it is of great importance to find a set of invariants that is not affected by blurring. This is the objective of this paper.

The first paper on this subject was reported by Flusser and Suk [15] who derived invariants to convolution with an arbitrary centrosymmetric PSF. These invariants have been successfully used in pattern recognition [22]–[25], in blurred digit and character recognition [26], [27], in medical image registration [28], and in focus/defocus quantitative measurement [29]. Other sets of blur invariants have been derived for some particular kinds of PSF like the axisymmetric blur invariants [30] and motion blur invariants [31], [32]. More recently, Flusser and Zitova introduced the combined blur-rotation invariants [33] and applied them to satellite image registration [34] and camera motion estimation [35]. Zhang et al. [36] proposed a method to get a set of affine-blur invariants. However, in their approach, the affine invariance is achieved through a normalization process. Suk and Flusser derived explicitly a set of combined invariants with respect to affine transform and to blur [37]. These blur invariants have been further extended to N -dimensions in continuous case [38] as well as in discrete form [39]. The above mentioned methods are mainly based on geometric or complex moments. The resulting invariants have information redundancy and are more sensitive to noise.

We [40] have recently proposed an approach based on the orthogonal Legendre moments to derive a set of blur invariants, and we have shown that they are more robust to noise and have better discriminative power than the existing methods. However, as pointed out in [40], one weak point of Legendre moment descriptors is that they are only invariant to translation, but not invariant under image rotation

and scaling. Zhu et al. [41] and Ji and Zhu [42] proposed the use of the Zernike moments to construct a set of combined blur-rotation invariants. Unfortunately, there are two limitations to their methods: (1) Only the Gaussian blur has been taken into account, which is a special case of PSF having circular symmetry; (2) Only a subset of Zernike moments of order p with repetition p , $Z_{p,p}$, has been used in the derivation of invariants. Since $Z_{p,p}$ corresponds to the radial moment $D_{p,p}$ or the complex moment $C_{0,p}$ if neglecting the normalization factor, the set of invariants constructed by Zhu et al. is a subset of that proposed by Flusser [43].

In this paper, we propose a new method to derive a set of combined geometric-blur invariants based on orthogonal Zernike moments. We further assume that the applied PSF is circularly symmetric. The reasons for such a choice of PSF are as follows [43]: (1) The majority of the PSFs occurring in real situations exhibit a circular symmetry; (2) Since the PSFs having circular symmetry are a subset of centrosymmetric functions, it could be expected that we can derive some new invariants. In fact, the previously reported convolution invariants with centrosymmetric PSF include only the odd order moments. Flusser and Zitova [43] have shown that there exist even order moment invariants with circularly symmetric PSF.

The organization of this paper is as follows. In Section II, some preliminaries about the radial moments, Zernike moments and image blurring are given. In Section III, we first establish a relationship between the Zernike moments of the blurred image and those of the original image and the PSF, and we then explain how to construct a set of blur invariants and joint radiometric-geometric invariants. Experimental results on the proposed descriptors' performance are provided in Section IV. Section V concludes the paper.

Preliminaries

This section presents the definition of radial and Zernike moments, and reviews the concept of image blurring. The radial moment of order p with repetition q of image intensity function $f(r, \theta)$ is defined as [44]

$$D_{p,q}^{(f)} = \int_0^{2\pi} \int_0^1 r^p e^{-jq\theta} f(r, \theta) r dr d\theta, \quad \hat{j} = \sqrt{-1}, \quad 0 \leq r \leq 1, \quad p \geq 0, \quad q = 0, \pm 1, \pm 2, \dots$$

The Zernike moment of order p with repetition q of $f(r, \theta)$ is defined as [44]

$$Z_{p,q}^{(f)} = \frac{p+1}{\pi} \int_0^{2\pi} \int_0^1 R_{p,q}(r) e^{-jq\theta} f(r, \theta) r dr d\theta, \quad p \geq 0, \quad |q| \leq p, \quad p - |q| \text{ being even,}$$

where $R_{p,q}(r)$ is the real-valued radial polynomial given by

$$R_{p,q}(r) = \sum_{k=0}^{(p-|q|)/2} \frac{(-1)^k (p-k)!}{k! \left(\frac{p+q}{2} - k\right)! \left(\frac{p-q}{2} - k\right)!} r^{p-2k}.$$

Equation (3) points out that the radial polynomial $R_{p,q}(r)$ is symmetric with q , that is, $R_{p,-q}(r) = R_{p,q}(r)$, for $q \geq 0$. Thus, we can consider the case where $q \geq 0$. Letting $p = q + 2l$ in (3) with $l \geq 0$, and substituting it into (2) yields

$$\begin{aligned} Z_{q+2l,q}^{(f)} &= \frac{q+2l+1}{\pi} \int_0^{2\pi} \int_0^1 \left[\sum_{k=0}^l (-1)^k \frac{(q+2l-k)!}{k!(q+l-k)!(l-k)!} r^{q+2l-2k} \right] e^{-jq\theta} f(r, \theta) r dr d\theta \\ &= \frac{q+2l+1}{\pi} \int_0^{2\pi} \int_0^1 \left[\sum_{k=0}^l (-1)^{l-k} \frac{(q+l+k)!}{k!(q+k)!(l-k)!} r^{q+2k} \right] e^{-jq\theta} f(r, \theta) r dr d\theta \\ &= \sum_{k=0}^l (-1)^{l-k} \frac{q+2l+1}{\pi} \frac{(q+l+k)!}{k!(q+k)!(l-k)!} \int_0^{2\pi} \int_0^1 r^{q+2k} e^{-jq\theta} f(r, \theta) r dr d\theta \\ &= \sum_{k=0}^l C_{l,k}^q D_{q+2k,q}^{(f)} \end{aligned}$$

where

$$C_{l,k}^q = (-1)^{l-k} \frac{q+2l+1}{\pi} \frac{(q+l+k)!}{k!(l-k)!(q+k)!}.$$

Let f' be a rotated version of f , i.e. $f'(r, \theta) = f(r, \theta - \beta)$, where β is the angle of rotation, and let $Z_{q+2l, q}^{(f')}$ be the Zernike moments of f' . It can be easily seen from (2) that

$$Z_{q+2l, q}^{(f')} = e^{-j\hat{j}q\beta} Z_{q+2l, q}^{(f)}$$

Let $g(x, y)$ be a blurred version of the original image $f(x, y)$, under the condition that of imaging system being linear shift-invariant, the blurring can be usually described by the convolution

$$g(x, y) = (f * h)(x, y)$$

where $h(x, y)$ is the PSF of the imaging system, and $*$ denotes the linear convolution.

In this paper, we assume that the PSF, $h(x, y)$, is a circularly symmetric image function, and that the imaging system is energy-preserving, which leads to,

$$\begin{aligned} h(x, y) &= h(r, \theta) = h(r) \\ \iint h(x, y) dx dy &= 1. \end{aligned}$$

Under the assumption of (8), the Zernike moments of $h(r, \theta)$ equal those of any rotated image h' . Combining this fact with (6), we get

$$Z_{q+2l, q}^{(h)} = Z_{q+2l, q}^{(h')} = e^{-j\hat{j}q\beta} Z_{q+2l, q}^{(h)}$$

Equation (10) is verified if and only if either $Z_{q+2l, q}^{(h)} = 0$ or $q = 0$. Thus, an important property of circularly symmetric functions can be stated as follows.

Proposition 1

If $q \neq 0$ and $h(r, \theta)$ is a circularly symmetric image function, then $Z_{q+2l, q}^{(h)} = 0$ for any non-negative integer l .

Method

Zernike Moments of the Blurred Image

In this subsection, we establish the relationship between the Zernike moments of the blurred image and those of the original image and the PSF. To that end, we first consider the radial moments. Applying (1) to blurred image $g(x, y)$, we have

$$\begin{aligned} D_{q+2k, q}^{(g)} &= \int_{-\infty}^{\infty} \int_{-\infty}^{\infty} (x - \hat{j}y)^{q+k} (x + \hat{j}y)^k g(x, y) dx dy \\ &= \int_{-\infty}^{\infty} \int_{-\infty}^{\infty} (x - \hat{j}y)^{q+k} (x + \hat{j}y)^k \left[\int_{-\infty}^{\infty} \int_{-\infty}^{\infty} h(a, b) f(x-a, y-b) da db \right] dx dy \\ &= \int_{-\infty}^{\infty} \int_{-\infty}^{\infty} h(a, b) \left[\int_{-\infty}^{\infty} \int_{-\infty}^{\infty} ((x - \hat{j}y) + (a - \hat{j}b))^{q+k} ((x + \hat{j}y) + (a + \hat{j}b))^k f(x, y) dx dy \right] da db \\ &= \sum_{m=0}^{q+k} \sum_{n=0}^k \binom{q+k}{m} \binom{k}{n} \int_{-\infty}^{\infty} \int_{-\infty}^{\infty} (x - \hat{j}y)^m (x + \hat{j}y)^n f(x, y) dx dy \int_{-\infty}^{\infty} \int_{-\infty}^{\infty} (a - \hat{j}b)^{q+k-m} (a + \hat{j}b)^{k-n} h(a, b) da db \\ &= \sum_{m=0}^{q+k} \sum_{n=0}^k \binom{q+k}{m} \binom{k}{n} D_{m+n, m-n}^{(f)} D_{q+2k-m-n, q+n-m}^{(h)} \end{aligned}$$

Applying (4) to blurred image $g(x, y) = g(r, \theta)$ and using (11), we obtain

$$Z_{q+2l, q}^{(g)} = \sum_{k=0}^l \sum_{m=0}^{q+k} \sum_{n=0}^k \binom{q+k}{m} \binom{k}{n} C_{l, k}^q D_{m+n, m-n}^{(f)} D_{q+2k-m-n, q+n-m}^{(h)}$$

From (4), the radial moments can also be expressed as a series of Zernike moments

$$D_{q+2l,q}^{(f)} = \sum_{k=0}^l d_{l,k}^q Z_{q+2k,q}^{(f)}$$

where $D_i^q = (d_{ij}^q)$, $0 \leq j \leq i \leq l$, is the inverse matrix of $C_i^q = (c_{ij}^q)$. Both C_i^q and D_i^q are lower triangular matrices of size $(l+1) \times (l+1)$, the elements of C_i^q are given by (5). The elements of D_i^q are given by [45]

$$d_{ij}^q = \frac{i!(q+i)! \pi}{(i-j)!(q+i+j+1)!}, \quad 0 \leq j \leq i \leq l.$$

From (13), we have

$$D_{m+n,m-n}^{(f)} = \sum_{i=0}^n d_{ni}^{m-n} Z_{m-n+2i,m-n}^{(f)}$$

$$D_{q+2k-m-n,q+n-m}^{(n)} = \sum_{j=0}^{k-n} d_{k-n,j}^{q+n-m} Z_{q+n-m+2j,q+n-m}^{(n)}$$

By introducing (15) and (16) into (12), we obtain

$$Z_{q+2l,q}^{(g)} = \sum_{k=0}^l \sum_{m=0}^{q+k} \sum_{n=0}^k \sum_{i=0}^n \sum_{j=0}^{k-n} \binom{q+k}{m} \binom{k}{n} c_{i,k}^q d_{ni}^{m-n} d_{k-n,j}^{q+n-m} Z_{m-n+2i,m-n}^{(f)} Z_{q+n-m+2j,q+n-m}^{(n)}$$

Based on (17), we have the following theorem.

Theorem 1

Let $f(r, \theta)$ be the original image function and the PSF $h(r, \theta)$ be circularly symmetric, $g(r, \theta)$ be a blurred version of $f(r, \theta)$, then the following relation

$$Z_{q+2l,q}^{(g)} = \sum_{i=0}^l Z_{q+2i,q}^{(f)} \sum_{j=0}^{l-i} Z_{2j,0}^{(n)} A(q, l, i, j)$$

stands for any $q \geq 0$ and $l \geq 0$, where the coefficients $A(q, l, i, j)$ are given by

$$A(q, l, i, j) = \sum_{k=i+j}^l \sum_{n=i}^{k-j} \binom{q+k}{q+n} \binom{k}{n} c_{i,k}^q d_{ni}^q d_{k-n,j}^0$$

Proof

For circularly symmetric function $h(r, \theta)$, using Proposition 1, we have $Z_{q+n-m+2j,q+n-m}^{(n)} = 0$ if $q+n-m \neq 0$, thus, (17) can be simplified as

$$Z_{q+2l,q}^{(g)} = \sum_{k=0}^l \sum_{n=0}^k \sum_{i=0}^n \sum_{j=0}^{k-n} \binom{q+k}{q+n} \binom{k}{n} c_{i,k}^q d_{ni}^q d_{k-n,j}^0 Z_{q+2i,q}^{(f)} Z_{2j,0}^{(n)}$$

$$= \sum_{i=0}^l Z_{q+2i,q}^{(f)} \sum_{j=0}^{l-i} Z_{2j,0}^{(n)} \sum_{k=i+j}^l \sum_{n=i}^{k-j} \binom{q+k}{q+n} \binom{k}{n} c_{i,k}^q d_{ni}^q d_{k-n,j}^0$$

The proof has been completed.

Blur Invariants of Zernike Moments

Based on Theorem 1, it becomes possible to construct a set of blur invariants of Zernike moments which is described in the following theorem.

Theorem 2

Let $f(r, \theta)$ be an image function. Let us define the following function $\mathbf{I}^{(f)}: \mathbf{N} \times \mathbf{N} \rightarrow \mathbf{R}$

$$I(q+2l, q)^{(f)} = Z_{q+2l, q}^{(f)} - \frac{1}{Z_{0,0}^{(f)}\pi} \sum_{i=0}^{l-1} I(q+2i, q)^{(f)} \sum_{j=0}^{l-i} Z_{2j,0}^{(f)} A(q, l, i, j)$$

Then, $I(q+2l, q)^{(f)}$ is invariant to circularly symmetric blur for any $q \geq 0$ and $l \geq 0$. The number $p = q+2l$ is called the order of the invariant.

The proof of Theorem 2 is given in Appendix A . Some remarks deserve to be made.

Remark 1

By using the symmetric property of $R_p, q(r)$ with q , it can be easily proven that $I(|q|+2l, q)^{(f)}$ for $q < 0$ is also invariant to convolution.

Remark 2

It can be deduced from (20) that $I(2l, 0)^{(f)} = (-1)^l (2l+1) Z_{0,0}^{(f)}$. Thus, only $I(0, 0)^{(f)} = Z_{0,0}^{(f)}$ will be used as invariant for the case $q = 0$.

Remark 3

If we use the Zernike central moments $Z_{q+2l, q}^{(f)}$ instead of Zernike moments in (20), then we can obtain a set of invariants $I(q+2l, q)^{(f)}$ that is invariant to both translation and to blur.

Based on Theorem 2, we can construct a set of blur invariants of Zernike moments with arbitrary order and express them in explicit form. The invariants up to sixth order are listed in Appendix B .

Lemma 1

Let f' be a rotated version of f , i.e., $f'(r, \theta) = f(r, \theta - \beta)$, where β denotes the rotation angle, then the following relation holds for any $q \geq 0$ and $l \geq 0$

$$I(q+2l, q)^{(f')} = e^{-j\alpha\beta} I(q+2l, q)^{(f)}$$

Proof

We demonstrate this lemma by induction about l . The proof is trivial for $l = 0$. Assume that the assertion is true for $1, 2, \dots, l-1$, then using (6), we get

$$\begin{aligned} I(q+2l, q)^{(f')} &= Z_{q+2l, q}^{(f')} - \frac{1}{Z_{0,0}^{(f')}\pi} \sum_{i=0}^{l-1} I(q+2i, q)^{(f')} \sum_{j=0}^{l-i} Z_{2j,0}^{(f')} A(q, l, i, j) \\ &= e^{-j\alpha\beta} Z_{q+2l, q}^{(f)} - \frac{1}{Z_{0,0}^{(f)}\pi} \sum_{i=0}^{l-1} e^{-j\alpha\beta} I(q+2i, q)^{(f)} \sum_{j=0}^{l-i} Z_{2j,0}^{(f)} A(q, l, i, j) \\ &= e^{-j\alpha\beta} I(q+2l, q)^{(f)}. \end{aligned}$$

The proof is thus completed

Lemma 2

Let $f(r, \theta)$ be an image function. It holds for any $q \geq 0$ and $l \geq 0$ that

$$I(q+2l, -q)^{(f)} = I^*(q+2l, q)^{(f)}$$

where the superscript $*$ denotes the complex conjugate.

The proof of Lemma 2 is very similar to that of Lemma 1 and it is thus omitted.

Combined Invariants of Zernike Moments

In this subsection, we construct a set of combined geometric-blur invariants. As we have already stated, the translation invariance can be achieved by using the central Zernike moments. Equation (21) shows that the magnitude of $I(q+2l, q)^{(f)}$ is invariant to rotation. However, as indicated by Flusser [33], the magnitudes do not yield a complete set of the invariants. Herein, we provide a way to build up such a set. Let f' and f be two images having the same content but distinct orientation (π) and scale (λ), that is, $f'(r, \theta) = f(r/\lambda, \theta - \beta)$, the Zernike moment of the transformed image is given by

$$\begin{aligned} Z_{q+2l, q}^{(f')} &= \frac{q+2l+1}{\pi} \int_0^{2\pi} \int_0^1 R_{q+2l, q}(r) e^{-j q \theta} f(r/\lambda, \theta - \beta) r dr d\theta \\ &= e^{-j q \beta} \frac{q+2l+1}{\pi} \lambda^2 \int_0^{2\pi} \int_0^1 R_{q+2l, q}(\lambda r) e^{-j q \theta} f(r, \theta) r dr d\theta. \end{aligned}$$

Using (4) and (13), we have

$$\begin{aligned} Z_{q+2l, q}^{(f')} &= e^{-j q \beta} \sum_{k=0}^l \lambda^{q+2k+2} C_{l, k}^q D_{q+2k, q}^{(f)} \\ &= e^{-j q \beta} \sum_{k=0}^l \sum_{m=0}^k \lambda^{q+2k+2} C_{l, k}^q d_{k, m}^q Z_{q+2m, q}^{(f)} \\ &= e^{-j q \beta} \sum_{m=0}^l \sum_{k=m}^l \lambda^{q+2k+2} C_{l, k}^q d_{k, m}^q Z_{q+2m, q}^{(f)} \end{aligned}$$

Therefore, we have the following theorem:

Theorem 3

Let

$$L_{q+2l, q}^{(f)} = e^{-j q \theta_f} \sum_{m=0}^l \sum_{k=m}^l \Gamma_f^{-(q+2k+2)} C_{l, k}^q d_{k, m}^q Z_{q+2m, q}^{(f)}$$

with $\theta_f = \arg(Z_{10}^{(f)})$ and $\Gamma_f = \sqrt{Z_{00}^{(f)}}$. Then $L_{q+2l, q}^{(f)}$ is invariant to both image rotation and scaling for any non-negative integers q and l .

The proof of Theorem 3 is given in Appendix A.

Remark 4

Many other choices of θ_f and Γ_f are possible. In fact, they can be chosen in such a way that $\Gamma_{f'} = \lambda \Gamma_f$, $\theta_{f'} = \theta_f - \beta$ where $f'(r, \theta) = f(r/\lambda, \theta - \beta)$ is the transformed image of f . However, it is preferable to use the lower order moments because they are less sensitive to noise than the higher order ones [46]. If the central moments are used, θ_f can be chosen as $\theta_f = \arg(Z_{30}^{(f)})$.

Theorem 4

For any $q \geq 0$ and $l \geq 0$, let

$$SI(q+2l, q)^{(f)} = e^{-j q \theta_f} \sum_{m=0}^l \sum_{k=m}^l \Gamma_f^{-(q+2k+2)} C_{l, k}^q d_{k, m}^q I(q+2m, q)^{(f)},$$

where $I(q+2m, q)^{(f)}$ is defined in (20). Then, $SI(q+2l, q)^{(f)}$ is both invariant to convolution and to image scaling and rotation. The proof is given in appendix A. For simplicity, the invariants defined in (26) are hereafter denoted by ZMIs. The combined invariants up to sixth order are listed in Appendix C.

Experimental Results

The following experiments illustrate the invariance of our ZMIs to various PSFs and similarity transformation, as its robustness to different kinds of noise. Comparison with existing methods in terms of recognition accuracy and template matching is also provided.

Let $SI_p = \{SI(p, p-2 \times \lfloor \frac{p-1}{2} \rfloor), SI(p, p+2-2 \times \lfloor \frac{p-1}{2} \rfloor), \dots, SI(p, p)\}$ for $P \geq 0$, where $SI(p, q)$ is defined in (26) and $\lfloor x \rfloor$ denotes the nearest integers not greater than x , and let $\mathbf{I}(p) = (SI_0, SI_1, \dots, SI_p)$. The relative error between the two moment invariant vectors corresponding to an image f and its transformed version g is computed by

$$E_p(f, g) = \frac{\|\tilde{I}^{(f)}(p) - \tilde{I}^{(g)}(p)\|}{\|\tilde{I}^{(f)}(p)\|},$$

where $\|\cdot\|$ is Euclidean norm in L^2 space.

Test of Invariance

For this experiment, a set of eighteen butterfly images shown in Fig. 1, whose size is 128×128 , has been chosen from the public Butterfly database [47] as the original images. In order to evaluate the invariance with respect to rotation and blurring, these images were rotated by different angles from 0° to 90° every 5° , and a bilinear interpolation was used when required. Then, the normalized uniform disk blur with different sizes from 1×1 (no blurring) to 31×31 with interval 2 (sixteen masks in total) was applied to every rotated image. So, the actual size of the blurred images in the experiments of this subsection is 212×212 . Note that the original images have been zero padded to meet the actual size in order to avoid the boundary effect. Both the original images and the blurred images are then mapped inside the unit circle, and the Zernike moments are computed with the method reported in [48]. The combined rotation-blur invariants ZMIs defined in (26) of order up to $p = 5$ were computed for all 5472 images. The relative errors of ZMIs between each transformed image and its original image were computed using (27). Fig. 2 shows the mean values of $E_p(f_i, g_i)$ where f_i ($i = 1, 2, \dots, 18$) denotes the images shown in Fig. 1 (a)–(r). It can be seen that they are very low (less than 0.0035). The mean relative error reaches its maximal value at the angle $\beta = 45^\circ$ due to the interpolation effect. The maximal value of the standard deviation (STD) is equal to 0.0035. We then tested the combined scale-blur invariance. Eighteen images were blurred with the same masks, and then were scaled by a factor varying from 0.5 to 2 with interval 0.1, forming a set of 4608 images. Fig. 3 shows the mean values of the relative errors $E_p(f_i, g_i)$ ($i = 1, 2, \dots, 18$) (the maximal value of the standard deviation is 0.0043). It can be observed from Figs. 2 and 3 that the errors caused by blurring and similarity transformation are very small (less than 0.006).

In the second experiment, the image shown in Fig. 1 (a) was convoluted with various PSFs and undergone similarity transformation including translation, scaling and rotation (Fig. 4). The proposed ZMIs defined in (26) of order p from 2 to 5 were calculated for each image (the central Zernike moments were used in this experiment, and the moment invariants of order 0 and 1 were respectively used to achieve the scale invariance and translation invariance). Table 1 depicts the invariant values. From this table, it can be seen that excellent results have been obtained whatever the similarity transformation and image degradation.

We also compared our ZMIs with the complex moment invariants (CMIs) reported in [43] and the Legendre moment invariants (LMIs) presented in [40] in terms of blur invariance. This is because these methods have different behavior regarding to similarity transformation: LMIs are invariant to translation only and CMIs are invariant to rotation and scaling. We do not include Zhu's method in this comparison due to the fact that the set of invariants derived in [41], [42] is a subset of both CMIs and ZMIs. Eighteen images were degraded by the normalized uniform disk blur with sixteen different sizes from 1×1 to 31×31 . Three types of blur invariants of order up to $p = 5$ are calculated for the set of 288 images. The mean values of the relative errors $E_p(f_i, g_i)$ ($i = 1, 2, \dots, 18$) for CMIs, LMIs and ZMIs are depicted in Fig. 5. It is clear that the errors increase significantly with the size of the mask going up and our ZMIs behave better than the two other types blur invariants.

Classification Results

In this evaluation, we also use the images shown in Fig. 1. The testing set was generated by adding disk blur, averaging blur and Gaussian blur with zero-mean and $STD = 1, 2$. The mask with sizes $3 \times 3, 5 \times 5, 7 \times 7, \dots, 17 \times 17, 19 \times 19$ pixels has been used, forming a set of 648 images. This was followed by adding a white Gaussian noise with different standard deviations and salt-and-pepper noise with different noise densities. Because the actual size of the PSF is usually unknown in practical application, in order to evaluate the performance of the different methods under such a situation, we take the size of the blurred image equal to the original image one (128×128) instead of its actual size (146×146) in this experiment even if the size of the mask is given. In that case, the boundary effect is then present. Fig. 6 shows some examples of the blurred and corrupted images. The Lance-Williams distance is used here as the classification measure. This distance between the two images f and g is defined by their moment invariant vectors $\gamma^{(f)} = (I_1^{(f)}, I_2^{(f)}, \dots, I_n^{(f)})$ and $\gamma^{(g)} = (I_1^{(g)}, I_2^{(g)}, \dots, I_n^{(g)})$ as

$$d(f, g) = \frac{1}{n} \sum_{j=1}^n \frac{|I_j^{(f)} - I_j^{(g)}|}{|I_j^{(f)}| + |I_j^{(g)}|},$$

where $I_j^{(f)}, j = 1, 2, \dots, n$, denote the blur invariants, n is the total number of invariants used in the experiment and $|x|$ the magnitude of the complex number x .

We have computed the ZMIs, CMIs and LMIs up to order $M = 1, 3, \dots, 15, 17$. The mean classification rates under different noise conditions for different values of M are shown in Fig. 7. It can be observed that the rate first increases, reaches the maximum value and

then decreases for all three methods. In other words, there should exist an optimal order for each type of moment invariants. This behaviour has also been observed and pointed out by Liao and Pawlak in image reconstruction due to the noise influence [49]. In this experiment, the optimal order for CMIs is $M = 7$ (the feature vector includes 17 invariants), $M = 7$ for LMIs (the feature vector has 21 invariants), and $M = 9$ for ZMIs (with 26 invariants). Table 2 shows the detailed classification rates using the different moment invariants with the optimal order. One can see from this table that in the noise-free scenario the recognition results are quite good whatever the method. The classification rates remain high for low and moderate noise levels but decrease significantly when the noise level goes up. However, the proposed descriptors ZMIs perform better than other methods (all the rates are higher than 75%) whatever the noise and the noise level. Although this conclusion is drawn from only one experiment, it is in accordance with that reported in [50] where the authors pointed out that the Zernike moments have an overall better performance than other moments.

Template Matching

The objective of this additional test is to evaluate the performance of our descriptors in the case of localizing templates within a real outdoor scene image that has undergone similarity transformation and out-of-focus blur. For that purpose, two images were taken by digital camera (Panasonic DMC-FZ50) with different focus and different positions by rotating the camera. Then, nine circular areas with radius $r = 10$ pixels were extracted from Fig. 8 (a) to serve as templates (numbered from 1 to 9). The scale factor between two images is obtained with the automatic scale selection [51]. After that, the scaled template was shifted across the transformed and blurred image (Fig. 8 (b)). At each position, the invariants were calculated and compared with the invariants of the original template. For more detail about the matching procedure, we refer to Ref. [22].

Each moment descriptors with the optimal order obtained in the previous experiment ($M = 9$ for ZMIs and $M = 7$ for CMIs) have been used here. Note that we did not test LMIs because they are not invariant with respect to image rotation and scaling. The 'matching position' we consider corresponds to the location where the Lance-Williams distance $d(f, g)$ reaches the minimum value, with f representing the template of the original image and g the template of the transformed and blurred image. The matching results that have been obtained based on these different moment invariants are summarized in Fig. 8 (c) and (d). It can be seen that the proposed descriptors ZMIs match correctly for all nine templates and that it is not the case for CMIs.

Conclusions

In this paper, we have proposed a method to construct a set of combined geometric-blur invariants using the orthogonal Zernike moments. The relationship between the Zernike moments of the blurred image and those of the original image and the PSF has been established. Based on this relationship, a set of invariants to convolution with circularly symmetric PSF has been derived. The advantages of the proposed method over the existing ones are the following: (1) The proposed descriptors are simultaneously invariant to similarity transformation and to convolution. Using these invariants, the image deblurring and geometric normalization process can be well avoided; (2) Like the method reported in [43], our method can also derive the even order invariants. The experiments conducted so far in very distinct situations demonstrated that the proposed descriptors are more robust to noise and have better discriminative power than the existing methods.

Appendix A

Proof of Theorem 2

We prove this theorem by mathematical induction about l .

For $l = 0$, using (18), (19) and $Z_{00}^{(n)} = 1/\pi$, it can be easily deduced from (20) that

$$I(q, q)^{(g)} = Z_{q,q}^{(g)} = Z_{q,q}^{(f)} = I(q, q)^{(f)}.$$

Assume that Theorem 1 is valid for $1, 2, \dots, l-1$, then we get

$$I(q+2l, q)^{(g)} - I(q+2l, q)^{(f)} = (Z_{q+2l,q}^{(g)} - Z_{q+2l,q}^{(f)}) - \frac{1}{Z_{00}^{(f)} \pi} \sum_{i=0}^{l-1} I(q+2i, q)^{(f)} \sum_{j=1}^{l-i} [Z_{2j,0}^{(g)} - Z_{2j,0}^{(f)}] A(q, l, i, j)$$

By using (18), we have

$$Z_{q+2l,q}^{(g)} - Z_{q+2l,q}^{(f)} = \sum_{i=0}^{l-1} Z_{q+2i,q}^{(f)} \sum_{j=0}^{l-i} Z_{2j,0}^{(g)} A(q, l, i, j)$$

Similarly,

$$Z_{2j,0}^{(g)} - Z_{2j,0}^{(f)} = \sum_{k=0}^{j-1} Z_{2k,0}^{(f)} \sum_{r=0}^{j-k} Z_{2r,0}^{(h)} A(0, j, k, r)$$

Substitution of (A2) and (A3) into (A1) yields

$$I(q+2l, q)^{(g)} - I(q+2l, q)^{(f)} = \sum_{j=0}^{l-1} Z_{q+2i,q}^{(f)} \sum_{j=0}^{l-i} Z_{2j,0}^{(h)} A(q, l, i, j) - \frac{1}{Z_{0,0}^{(f)} \pi} \sum_{i=0}^{l-1} I(q+2i, q)^{(f)} \sum_{j=0}^{l-i} \left[\sum_{k=0}^{j-1} Z_{2k,0}^{(f)} \sum_{r=0}^{j-k} Z_{2r,0}^{(h)} A(0, j, k, r) \right] A(q, l, i, j)$$

By using the property $c_{ij}^a d_{ij}^a = 1$ and $d_{00}^a = \pi$, (20) can be written as

$$Z_{q+2l,q}^{(f)} = \frac{1}{Z_{0,0}^{(f)} \pi} \sum_{i=0}^l I(q+2i, q)^{(f)} \sum_{j=0}^{l-i} Z_{2j,0}^{(h)} A(q, l, i, j)$$

Substitution of (A5) into (A4), we get

$$\begin{aligned} & I(q+2l, q)^{(g)} - I(q+2l, q)^{(f)} \\ &= \sum_{i=0}^{l-1} \left[\frac{1}{Z_{0,0}^{(f)} \pi} \sum_{k=0}^i I(q+2k, q)^{(f)} \sum_{r=0}^{i-k} Z_{2r,0}^{(f)} A(q, i, k, r) \right] \sum_{j=0}^{l-i} Z_{2j,0}^{(h)} A(q, l, i, j) \\ & - \frac{1}{Z_{0,0}^{(f)} \pi} \sum_{i=0}^{l-1} I(q+2i, q)^{(f)} \sum_{j=0}^{l-i} \left[\sum_{k=0}^{j-1} Z_{2k,0}^{(f)} \sum_{r=0}^{j-k} Z_{2r,0}^{(h)} A(0, j, k, r) \right] A(q, l, i, j) \\ &= \frac{1}{Z_{0,0}^{(f)} \pi} \sum_{k=0}^{l-1} I(q+2k, q)^{(f)} \sum_{i=k}^{l-1} \sum_{r=0}^{i-k} Z_{2r,0}^{(f)} A(q, i, k, r) \sum_{j=0}^{l-i} Z_{2j,0}^{(h)} A(q, l, i, j) \\ & - \frac{1}{Z_{0,0}^{(f)} \pi} \sum_{i=0}^{l-1} I(q+2i, q)^{(f)} \sum_{k=0}^{l-i-1} Z_{2k,0}^{(f)} \sum_{j=k+1}^{l-i} \sum_{r=0}^{j-k} Z_{2r,0}^{(h)} A(0, j, k, r) A(q, l, i, j) \\ &= \frac{1}{Z_{0,0}^{(f)} \pi} \sum_{k=0}^{l-1} I(q+2k, q)^{(f)} \sum_{r=0}^{l-1-k} Z_{2r,0}^{(f)} \sum_{j=0}^{l-k-r} Z_{2j,0}^{(h)} \sum_{i=k+r}^{\min(l-1, l-j)} A(q, i, k, r) A(q, l, i, j) \\ & - \frac{1}{Z_{0,0}^{(f)} \pi} \sum_{i=0}^{l-1} I(q+2i, q)^{(f)} \sum_{k=0}^{l-1-i} Z_{2k,0}^{(f)} \sum_{r=0}^{l-i-k} Z_{2r,0}^{(h)} \sum_{j=\max(k+r, k+1)}^{l-i} A(0, j, k, r) A(q, l, i, j) \end{aligned}$$

By shifting the indices in the above equation, we have

$$\begin{aligned} & I(q+2l, q)^{(g)} - I(q+2l, q)^{(f)} \\ &= \frac{1}{Z_{0,0}^{(f)} \pi} \sum_{i=0}^{l-1} I(q+2i, q)^{(f)} \sum_{j=0}^{l-1-i} Z_{2j,0}^{(f)} \sum_{k=0}^{l-i-j} Z_{2k,0}^{(h)} \sum_{r=i+j}^{\min(l-1, l-k)} A(q, r, i, j) A(q, l, r, k) \\ & - \frac{1}{Z_{0,0}^{(f)} \pi} \sum_{i=0}^{l-1} I(q+2i, q)^{(f)} \sum_{j=0}^{l-1-i} Z_{2j,0}^{(f)} \sum_{k=0}^{l-i-j} Z_{2k,0}^{(h)} \sum_{r=\max(j+k, j+1)}^{l-i} A(0, r, j, k) A(q, l, i, r) \\ &= \frac{1}{Z_{0,0}^{(f)} \pi} \sum_{i=0}^{l-1-i} I(q+2i, q)^{(f)} \sum_{j=0}^{l-1-i} Z_{2j,0}^{(f)} \sum_{k=0}^{l-i-j} Z_{2k,0}^{(h)} T(q, l, i, j, k) \end{aligned}$$

where

$$T(q, l, i, j, k) = \sum_{r=i+j}^{\min(l-1, l-k)} A(q, r, i, j)A(q, l, r, k) - \sum_{r=\max(j+k, j+1)}^{l-i} A(0, r, j, k)A(q, l, i, r)$$

By using (19), we have

$$A(q, l, l, 0) = A(0, j, j, 0),$$

(A8) can thus be rewritten as

$$\begin{aligned} & T(q, l, i, j, k) \\ &= \sum_{r=i+j}^{l-k} A(q, r, i, j)A(q, l, r, k) - \sum_{r=j+k}^{l-i} A(0, r, j, k)A(q, l, i, r) \\ &= \sum_{r=i+j}^{l-k} \sum_{m=i+j}^r \sum_{n=i}^{m-j} \sum_{s=r+k}^{m-j} \sum_{t=r}^{s-k} \binom{q+s}{q+t} \binom{s}{t} \binom{q+m}{q+n} \binom{m}{n} c_{l,s}^q c_{r,m}^q d_{n,i}^q d_{t,r}^q d_{s-t,k}^0 d_{m-n}^0 \\ &\quad - \sum_{r=j+k}^{l-i} \sum_{m=j+k}^r \sum_{n=j}^{m-k} \sum_{s=i+r}^{m-k} \sum_{t=i}^{s-r} \binom{q+s}{q+t} \binom{s}{t} \binom{m}{n} \binom{m}{n} c_{l,s}^q c_{r,m}^0 d_{t,i}^q d_{s-t,r}^0 d_{n,j}^0 d_{m-n,k}^0 \\ &= \sum_{s=i+j+k}^{l-i} c_{l,s}^q \sum_{r=i+j}^{s-k} \sum_{m=i+j}^r \sum_{n=i}^{m-j} d_{n,i}^q \sum_{t=r}^{s-k} \binom{q+s}{q+t} \binom{s}{t} \binom{q+m}{q+n} \binom{m}{n} d_{t,r}^q c_{r,m}^q d_{s-t,k}^0 d_{m-n}^0 \\ &\quad - \sum_{s=i+j+k}^{l-i} c_{l,s}^q \sum_{r=j+k}^{s-i} \sum_{t=i}^{s-r} d_{t,i}^q \sum_{m=j+k}^r \sum_{n=j}^{m-k} \binom{q+s}{q+t} \binom{s}{t} \binom{m}{n} \binom{m}{n} d_{s-t,r}^0 c_{r,m}^0 d_{m-n,k}^0 d_{n,j}^0 \\ &= \sum_{s=i+j+k}^{l-i} c_{l,s}^q \sum_{r=i}^{s-j-k} d_{n,i}^q \sum_{r=n+j}^{s-k} \sum_{m=n+j}^r \sum_{t=r}^{s-k} \binom{q+s}{q+t} \binom{s}{t} \binom{q+m}{q+n} \binom{m}{n} d_{t,r}^q c_{r,m}^q d_{s-t,k}^0 d_{m-n}^0 \\ &\quad - \sum_{s=i+j+k}^{l-i} c_{l,s}^q \sum_{t=i}^{s-j-k} d_{t,i}^q \sum_{r=j+k}^{s-t} \sum_{m=j+k}^r \sum_{n=j}^{m-k} \binom{q+s}{q+t} \binom{s}{t} \binom{m}{n} \binom{m}{n} d_{s-t,r}^0 c_{r,m}^0 d_{m-n,k}^0 d_{n,j}^0. \end{aligned}$$

By shifting the indices in the last part of the above equation, we get

$$\begin{aligned} & T(q, l, i, j, k) \\ &= \sum_{s=i+j+k}^{l-i} c_{l,s}^q \sum_{r=i}^{s-j-k} d_{n,i}^q \sum_{r=n+j}^{s-k} \sum_{m=n+j}^r \sum_{t=r}^{s-k} \binom{q+s}{q+t} \binom{s}{t} \binom{q+m}{q+n} \binom{m}{n} d_{t,r}^q c_{r,m}^q d_{s-t,k}^0 d_{m-n}^0 \\ &\quad - \sum_{s=i+j+k}^{l-i} c_{l,s}^q \sum_{r=i}^{s-j-k} d_{t,i}^q \sum_{r=j+k}^{s-n} \sum_{m=j+k}^r \sum_{t=j}^{m-k} \binom{q+s}{q+n} \binom{s}{n} \binom{m}{t} \binom{m}{t} d_{s-n,r}^0 c_{r,m}^0 d_{m-t,k}^0 d_{t,j}^0 \\ &= \sum_{s=i+j+k}^{l-i} c_{l,s}^q \sum_{r=i}^{s-j-k} d_{n,i}^q T_1(q, s, n, j, k) \end{aligned}$$

where

$$T_1(q, s, n, j, k) = \sum_{r=n+j}^{s-k} \sum_{m=n+j}^r \sum_{t=r}^{s-k} \binom{q+s}{q+t} \binom{s}{t} \binom{q+m}{q+n} \binom{m}{n} d_{t,r}^q c_{r,m}^q d_{s-t,k}^0 d_{m-n}^0 - \sum_{r=j+k}^{s-n} \sum_{m=j+k}^r \sum_{t=j}^{m-k} \binom{q+s}{q+n} \binom{s}{n} \binom{m}{t} \binom{m}{t} d_{s-n,r}^0 c_{r,m}^0 d_{m-t,k}^0 d_{t,j}^0$$

By changing the order of summation in (A12), we have

$$\begin{aligned} & T_1(q, s, n, j, k) \\ &= \sum_{r=n+j}^{s-k} \sum_{m=n+j}^r \sum_{t=r}^{s-k} \binom{q+s}{q+t} \binom{s}{t} \binom{q+m}{q+n} \binom{m}{n} d_{t,r}^q c_{r,m}^q d_{s-t,k}^0 d_{m-n}^0 - \sum_{r=j+k}^{s-n} \sum_{t=j}^{r-k} \sum_{m=t+k}^r \binom{q+s}{q+n} \binom{s}{n} \binom{m}{t} \binom{m}{t} d_{s-n,r}^0 c_{r,m}^0 d_{m-t,k}^0 \\ &= \sum_{r=n+j}^{s-k} \sum_{m=n+j}^r \binom{q+s}{q+t} \binom{s}{t} \binom{q+m}{q+n} \binom{m}{n} d_{s-t,k}^0 d_{m-n}^0 \left[\sum_{r=m}^t d_{t,r}^q c_{r,m}^q \right] - \sum_{t=j}^{s-n-k} \sum_{m=t+k}^{s-n} \binom{q+s}{q+n} \binom{s}{n} \binom{m}{t} \binom{m}{t} d_{m-t,k}^0 d_{t,j}^0 \left[\sum_{r=m}^{s-n} d_{s-r}^0 \right] \end{aligned}$$

Since the lower triangular matrix D_1^q is the inverse of the matrix C_1^q , that is, $D_1^q C_1^q = I$, where I is the identity matrix, we have $\sum_{m=0}^s \delta_{m,n} = \sum_{m=0}^s \delta_{m,n} = \delta_{m,n}$, where $\delta_{m,n}$ denotes the Kronecker symbol. Then, (A13) becomes

$$\begin{aligned}
T_1(q, s, n, j, k) &= \sum_{t=n+j}^{s-k} \binom{q+s}{q+t} \binom{s}{t} \binom{q+t}{q+n} \binom{t}{n} d_{s-t,k}^0 d_{t-n,j}^0 - \sum_{t=j}^{s-n-k} \binom{q+s}{q+n} \binom{s}{n} \binom{s-n}{t} \binom{s-n}{t} d_{s-n-t,k}^0 d_{t,j}^0 \\
&= \sum_{t=j}^{s-n-k} \binom{q+s}{q+n+t} \binom{s}{n+t} \binom{q+n+t}{q+n} \binom{n+t}{n} d_{s-n-t,k}^0 d_{t,j}^0 - \sum_{t=j}^{s-n-k} \binom{q+s}{q+t} \binom{s}{n} \binom{s-n}{t} \binom{s-n}{t} d_{s-n-t,k}^0 d_{t,j}^0 \\
&= \sum_{t=j}^{s-n-k} \frac{(q+s)!s}{n!(q+n)!(t!(s-n-t))^2} d_{s-n-t,k}^0 d_{t,j}^0 - \sum_{t=j}^{s-n-k} \frac{(q+s)!s}{n!(q+n)!(t!(s-n-t))^2} d_{s-n-t,k}^0 d_{t,j}^0 \\
&= 0.
\end{aligned}$$

Thus, $T(q, l, i, j, k) = 0$ and $I(q+2l, q)^{(s)} - I(q+2l, q)^{(t)} = 0$.

The proof has been completed.

Proof of Theorem 3

Equation (24) can be written in a matrix form as

$$\begin{pmatrix} Z_{a,q}^{f''} \\ Z_{q+2,q}^{f''} \\ \vdots \\ Z_{q+2l,q}^{f''} \end{pmatrix} = e^{-j\alpha\beta} C_1^q \text{diag}(\lambda^{q+2}, \lambda^{q+4}, \dots, \lambda^{q+2l+2}) D_1^q \begin{pmatrix} Z_{a,q}^f \\ Z_{q+2,q}^f \\ \vdots \\ Z_{q+2l,q}^f \end{pmatrix}.$$

Applying (25) to the transformed image f'' , it can also be expressed in a matrix form as

$$\begin{pmatrix} L_{a,q}^{f''} \\ L_{q+2,q}^{f''} \\ \vdots \\ L_{q+2l,q}^{f''} \end{pmatrix} = e^{-j\alpha\theta_f} C_1^q \text{diag}(\Gamma_f^{-(q+2)}, \Gamma_f^{-(q+4)}, \dots, \Gamma_f^{-(q+2l+2)}) D_1^q \begin{pmatrix} Z_{a,q}^{f''} \\ Z_{q+2,q}^{f''} \\ \vdots \\ Z_{q+2l,q}^{f''} \end{pmatrix}.$$

Based on the definition of Γ_f and θ_f , it can be easily verified that

$$\Gamma_{f''} = \lambda \Gamma_f, \quad \theta_{f''} = \theta_f - \beta.$$

Substitution of (A15) and (A17) into (A16), and using the identity $D_1^q C_1^q = I$, we obtain

$$\begin{aligned}
\begin{pmatrix} L_{a,q}^{f''} \\ L_{q+2,q}^{f''} \\ \vdots \\ L_{q+2l,q}^{f''} \end{pmatrix} &= e^{-j a \theta_r} C_1^q \text{diag}(\Gamma_f^{-(q+2)}, \Gamma_f^{-(q+4)}, \dots, \Gamma_f^{-(q+2l+2)}) \text{diag}(\lambda^{-(q+2)}, \lambda^{-(q+4)}, \dots, \lambda^{-(q+2l+2)}) D_1^q C_1^q \\
&\cdot \text{diag}(\lambda^{q+2}, \lambda^{q+4}, \dots, \lambda^{q+2l+2}) D_1^q \begin{pmatrix} Z_{a,q}^f \\ Z_{q+2,q}^f \\ \vdots \\ Z_{q+2l,q}^f \end{pmatrix} \\
&= e^{-j a \theta_r} C_1^q \text{diag}(\Gamma_f^{-(q+2)}, \Gamma_f^{-(q+4)}, \dots, \Gamma_f^{-(q+2l+2)}) D_1^q \begin{pmatrix} Z_{a,q}^f \\ Z_{q+2,q}^f \\ \vdots \\ Z_{q+2l,q}^f \end{pmatrix} \\
&= \begin{pmatrix} L_{a,q}^f \\ L_{q+2,q}^f \\ \vdots \\ L_{q+2l,q}^f \end{pmatrix}
\end{aligned}$$

The proof has been completed.

To prove Theorem 4, we need first the following Lemma.

Lemma 3

Let

$$CL(q+2l, q)^{(f)} = L_{q+2l,q}^{(f)} - \frac{1}{L_{0,0}^{(f)} \pi} \sum_{i=0}^{l-1} CL(q+2i, q)^{(f)} \sum_{j=0}^{l-i} L_{2j,0}^{(f)} A(q, l, i, j)$$

Then, $CL(q+2l, q)^{(f)}$ is invariant to image scaling and rotation for any $q \geq 0$ and $l \geq 0$.

Lemma 3 can be easily proven by mathematical induction and it is thus omitted.

Proof of Theorem 4

By Theorem 1, $I(q+2k, q)^{(f)}$ is invariant to convolution for any $q \geq 0$ and $k \geq 0$. Since $\Gamma_r = \sqrt{z_0^0}$ is also invariant to convolution, it is obvious that $SI(q+2l, q)^{(f)}$ defined in (26) is invariant to convolution. To demonstrate its invariance with respect to image scaling and rotation, we will prove the following result

$$SI(q+2l, q)^{(f)} = CL(q+2l, q)^{(f)},$$

where $CL(q+2l, q)^{(f)}$ is defined in (A19).

We demonstrate (A20) by mathematical induction about l .

For $l = 0$, using (A19), (20) and (25), we have

$$SI(q, q)^{(f)} = e^{-j a \theta_r} \Gamma_f^{-(q+2)} I(q, q)^{(f)} = e^{-j a \theta_r} \Gamma_f^{-(q+2)} Z_{a,q}^f = e^{-j a \theta_r} \Gamma_f^{-(q+2)} L_{a,q}^{(f)} = CL(q, q)^{(f)}.$$

Assume that the relationship (A20) is valid for $1, 2, \dots, l-1$. Then, using (20) and (25), we have

$$\begin{aligned}
& q+2l, q)^{(f)} \\
& e^{-j\varphi} \sum_{m=0}^l \sum_{k=m}^l \Gamma_f^{-(q+2k+2)} c_{l,k}^q d_{k,m}^q \left(Z_{q+2m,q}^{(f)} - \frac{1}{Z_{0,0}^{(f)} \pi} \sum_{i=0}^{m-1} I(q+2i, q)^{(f)} \sum_{j=0}^{m-i} Z_{2j,0}^{(f)} A(q, m, i, j) \right) \\
& e^{-j\varphi} \sum_{m=0}^l \sum_{k=m}^l \Gamma_f^{-(q+2k+2)} c_{l,k}^q d_{k,m}^q Z_{q+2m,q}^{(f)} - \frac{e^{-j\varphi}}{Z_{0,0}^{(f)} \pi} \sum_{m=0}^l \sum_{k=m}^l \Gamma_f^{-(q+2k+2)} c_{l,k}^q d_{k,m}^q \sum_{i=0}^{m-1} I(q+2i, q)^{(f)} \sum_{j=0}^{m-i} Z_{2j,0}^{(f)} A(q, m, i, j) \\
& L_{q+2l,q}^{(f)} - \frac{e^{-j\varphi} \Gamma_f^{-(q+2)}}{Z_{0,0}^{(f)} \pi} \sum_{i=0}^{l-1} I(q+2i, q)^{(f)} \sum_{j=0}^{l-i} Z_{2j,0}^{(f)} \sum_{m=\max(i,j,i+1)}^l \sum_{k=m}^l \Gamma_f^{-2k} c_{l,k}^q d_{k,m}^q A(q, m, i, j)
\end{aligned}$$

For $CL(q+2l, q)^{(f)}$, using the assumption $CL(q+2i, q)^{(f)} = SI(q+2i, q)^{(f)}$ for $i = 0, 1, \dots, l-1$, and (26) and (25), we deduce from (A19) that

$$\begin{aligned}
CL(q+2l, q)^{(f)} &= L_{q+2l,q}^{(f)} - \frac{1}{L_{0,0}^{(f)} \pi} \sum_{i=0}^{l-1} SI(q+2i, q)^{(f)} \sum_{j=0}^{l-i} L_{2j,0}^{(f)} A(q, l, i, j) \\
&= L_{q+2l,q}^{(f)} - \frac{1}{L_{0,0}^{(f)} \pi} \sum_{i=0}^{l-1} e^{-j\varphi} \sum_{m=0}^i \sum_{k=m}^i \Gamma_f^{-(q+2k+2)} c_{i,k}^q d_{k,m}^q I(q+2m, q)^{(f)} \sum_{j=0}^{l-i} \left(\sum_{r=0}^j \sum_{t=r}^j \Gamma_f^{-(2t+2)} c_{j,r}^0 d_{t,r}^0 Z_{2r,0}^{(f)} \right) A(q, l, i, j)
\end{aligned}$$

From (25), we have $L_{0,0}^{(f)} = \Gamma_f^{-2} Z_{0,0}^{(f)}$, (A23) becomes

$$\begin{aligned}
q+2l, q)^{(f)} &= L_{q+2l,q}^{(f)} - \frac{e^{-j\varphi} \Gamma_f^{-(q+2)}}{Z_{0,0}^{(f)} \pi} \sum_{i=0}^{l-1} \left(\sum_{m=0}^i \sum_{k=m}^i \Gamma_f^{-2k} c_{i,k}^q d_{k,m}^q I(q+2m, q)^{(f)} \right) \sum_{j=0}^{l-i} \left(\sum_{r=0}^j \sum_{t=r}^j \Gamma_f^{-2t} c_{j,t}^0 d_{t,r}^0 Z_{2r,0}^{(f)} \right) A(q, l, i, j) \\
q+2l, q)^{(f)} &- \frac{e^{-j\varphi} \Gamma_f^{-(q+2)}}{Z_{0,0}^{(f)} \pi} \sum_{m=0}^{l-1} I(q+2m, q)^{(f)} \sum_{r=0}^{l-m} Z_{2r,0}^{(f)} \sum_{i=m}^{\min(l-1, l-r)} \sum_{k=m}^i \Gamma_f^{-2k} c_{i,k}^q d_{k,m}^q \sum_{j=r}^{l-i} \sum_{t=r}^j \Gamma_f^{-2t} c_{j,t}^0 d_{t,r}^0 A(q, l, i, j) \\
q+2l, q)^{(f)} &- \frac{e^{-j\varphi} \Gamma_f^{-(q+2)}}{Z_{0,0}^{(f)} \pi} \sum_{i=0}^{l-1} I(q+2i, q)^{(f)} \sum_{j=0}^{l-i} Z_{2j,0}^{(f)} \sum_{m=i}^{\min(l-1, l-j)} \sum_{k=i}^m \Gamma_f^{-2k} c_{m,k}^q d_{k,i}^q \sum_{r=j}^{l-m} \sum_{t=j}^r \Gamma_f^{-2t} c_{j,t}^0 d_{t,j}^0 A(q, l, m, r).
\end{aligned}$$

Note that we have shifted the indices in the last step of the above equation. Subtracting (A22) from (A24), we obtain

$$\begin{aligned}
& -SI(q+2l, q)^{(f)} \\
& I(q+2i, q)^{(f)} \sum_{j=0}^{l-i} Z_{2j,0}^{(f)} \left[\sum_{m=\max(i,j,i+1)}^l \sum_{k=m}^l \Gamma_f^{-2k} c_{l,k}^q d_{k,m}^q A(q, m, i, j) - \sum_{m=i}^{\min(l-1, l-j)} \sum_{k=i}^m \Gamma_f^{-2k} c_{m,k}^q d_{k,i}^q \sum_{r=j}^{l-m} \sum_{t=j}^r \Gamma_f^{-2t} c_{j,t}^0 d_{t,j}^0 A(q, l, m, r) \right] \\
& I(q+2i, q)^{(f)} \sum_{j=0}^{l-i} Z_{2j,0}^{(f)} T(\Gamma_f, q, l, i, j)
\end{aligned}$$

where

$$T(\Gamma_f, q, l, i, j) = \sum_{m=\max(i,j,i+1)}^l \sum_{k=m}^l \Gamma_f^{-2k} c_{l,k}^q d_{k,m}^q A(q, m, i, j) - \sum_{m=i}^{\min(l-1, l-j)} \sum_{k=i}^m \Gamma_f^{-2k} c_{m,k}^q d_{k,i}^q \sum_{r=j}^{l-m} \sum_{t=j}^r \Gamma_f^{-2t} c_{j,t}^0 d_{t,j}^0 A(q, l, m, r)$$

For $j \geq 1$, (A26) becomes

$$T(\Gamma_f, q, l, i, j) = \sum_{m=i+1}^l \sum_{k=m}^l \Gamma_f^{-2k} c_{l,k}^q d_{k,m}^q A(q, m, i, j) - \sum_{m=i}^{l-j} \sum_{k=i}^m \Gamma_f^{-2k} c_{m,k}^q d_{k,i}^q \sum_{r=j}^{l-m} \sum_{t=j}^r \Gamma_f^{-2t} c_{j,t}^0 d_{t,j}^0 A(q, l, m, r)$$

For $j = 0$, (A26) becomes

$$\begin{aligned}
q, l, i, 0) &= \sum_{m=i+1}^l \sum_{k=m}^l \Gamma_f^{2k} c_{l,k}^q d_{k,m}^q A(q, m, i, 0) - \sum_{m=i}^{l-1} \sum_{k=i}^m \Gamma_f^{2k} c_{m,k}^q d_{k,i}^q \sum_{r=0}^{l-m} \sum_{t=0}^r \Gamma_f^{2t} c_{r,t}^0 d_{t,0}^0 A(q, l, m, r) \\
&= \sum_{m=i}^l \sum_{k=m}^l \Gamma_f^{2k} c_{l,k}^q d_{k,m}^q A(q, m, i, 0) - \sum_{m=i}^l \sum_{k=i}^m \Gamma_f^{2k} c_{m,k}^q d_{k,i}^q \sum_{r=0}^{l-m} \sum_{t=0}^r \Gamma_f^{2t} c_{r,t}^0 d_{t,0}^0 A(q, l, m, r)
\end{aligned}$$

Thus, (A26) can be rewritten as

$$\begin{aligned}
&(\Gamma_f, q, l, i, j) \\
&= \sum_{m=i+j}^l \sum_{k=m}^l \Gamma_f^{2k} c_{l,k}^q d_{k,m}^q A(q, m, i, j) - \sum_{m=i}^{l-j} \sum_{k=i}^m \Gamma_f^{2k} c_{m,k}^q d_{k,i}^q \sum_{r=j}^{l-m} \sum_{t=j}^r \Gamma_f^{2t} c_{r,t}^0 d_{t,j}^0 A(q, l, m, r) \\
&= \sum_{k=i+j}^l \Gamma_f^{2k} \sum_{m=i+j}^k c_{l,k}^q d_{k,m}^q A(q, m, i, j) - \sum_{k=i}^{l-j} \Gamma_f^{2k} \sum_{m=k}^{l-j} c_{m,k}^q d_{k,i}^q \sum_{t=j}^{l-m} \sum_{r=t}^{l-m} \Gamma_f^{2t} c_{r,t}^0 d_{t,j}^0 A(q, l, m, r) \\
&= \sum_{k=i+j}^l \Gamma_f^{2k} \sum_{m=i+j}^k c_{l,k}^q d_{k,m}^q A(q, m, i, j) - \sum_{k=i}^{l-j} \Gamma_f^{2k} \sum_{t=j}^{l-k} \Gamma_f^{2t} \sum_{m=k}^{l-t} c_{m,k}^q d_{k,i}^q \sum_{r=t}^{l-m} c_{r,t}^0 d_{t,j}^0 A(q, l, m, r) \\
&= \sum_{u=i+j}^l \Gamma_f^{2u} \sum_{m=i+j}^u c_{l,u}^q d_{u,m}^q A(q, m, i, j) - \sum_{u=i+j}^l \Gamma_f^{2u} \sum_{v=0}^{u-(i+j)} \sum_{m=i+v}^{l-u+i+v} \sum_{r=u-i-v}^{l-m} c_{m+i+v}^q d_{i+v,i}^q c_{r,u-i-v}^0 d_{u-i-v,j}^0 A(q, l, m, r) \\
&= \sum_{u=i+j}^l \Gamma_f^{2u} \left[\sum_{m=i+j}^u c_{l,u}^q d_{u,m}^q A(q, m, i, j) - \sum_{v=0}^{u-(i+j)} \sum_{m=i+v}^{l-u+i+v} \sum_{r=u-i-v}^{l-m} c_{m+i+v}^q d_{i+v,i}^q c_{r,u-i-v}^0 d_{u-i-v,j}^0 A(q, l, m, r) \right] \\
&= \sum_{u=i+j}^l \Gamma_f^{2u} T_1(q, l, i, j, u)
\end{aligned}$$

where

$$T_1(q, l, i, j, u) = \sum_{m=i+j}^u c_{l,u}^q d_{u,m}^q A(q, m, i, j) - \sum_{v=0}^{u-(i+j)} \sum_{m=i+v}^{l-u+i+v} \sum_{r=u-i-v}^{l-m} c_{m+i+v}^q d_{i+v,i}^q c_{r,u-i-v}^0 d_{u-i-v,j}^0 A(q, l, m, r)$$

By using (19) and the identity $D_i^q C_i^q = I$, (A30) can be written as

$$\begin{aligned}
& \sum_{m=k+i+j}^m \sum_{n=i}^{k-j} \binom{q+k}{q+n} \binom{k}{n} c_{m,k}^q d_{n,i}^q d_{k-n,j}^0 - \sum_{v=0}^{u-(i+j)} \sum_{m=i+v}^{l-u+i+v} \sum_{r=u-i-v}^{l-m} c_{m+i+v}^q d_{i+v,i}^q c_{r,u-i-v}^0 d_{u-i-v,j}^0 \sum_{k=m+i}^l \sum_{n=m}^{k-r} \binom{q+k}{q+n} \binom{k}{n} \\
& \binom{q+k}{q+n} \binom{k}{n} d_{n,i}^q d_{k-n,j}^0 \left[\sum_{m=k}^u d_{u,m}^q c_{m,k}^q \right] - \sum_{v=0}^{u-(i+j)} \sum_{m=i+v}^{l-u+i+v} \sum_{k=m+u-i-v}^l \sum_{r=i-i-v}^{k-m} \sum_{n=m}^{k-r} \binom{q+k}{q+n} \binom{k}{n} c_{l,k}^q d_{n,m}^q d_{k-n,r}^0 c_{m+i+v}^q d_{i+v,i}^q \\
& \binom{q+k}{q+n} \binom{k}{n} c_{l,u}^q d_{n,i}^q d_{u-n,j}^0 - \sum_{v=0}^{u-(i+j)} \sum_{k=i}^l \sum_{n=i+v}^{k-u+i+v} \binom{q+k}{q+n} \binom{k}{n} c_{l,k}^q d_{i+v,i}^q d_{u-i-v,j}^0 \left[\sum_{m=i+v}^n d_{n,m}^q c_{m+i+v}^q \right] \left[\sum_{r=i-i-v}^{k-n} d_{k-n,r}^0 c_{r,u-i-v}^0 \right] \\
& \binom{q+k}{q+n} \binom{k}{n} c_{l,u}^q d_{n,i}^q d_{u-n,j}^0 - \sum_{v=0}^{u-(i+j)} \sum_{k=i}^l \sum_{n=i+v}^{k-u+i+v} \binom{q+k}{q+n} \binom{k}{n} c_{l,k}^q d_{i+v,i}^q d_{u-i-v,j}^0 \left[\sum_{m=i+v}^n d_{n,m}^q c_{m+i+v}^q \right] \left[\sum_{r=i-i-v}^{k-n} d_{k-n,r}^0 c_{r,u-i-v}^0 \right] \\
& \binom{q+k}{q+n} \binom{k}{n} c_{l,u}^q d_{n,i}^q d_{u-n,j}^0 - \sum_{v=0}^{u-(i+j)} \binom{q+u}{q+i+v} \binom{u}{i+v} c_{l,u}^q d_{i+v,i}^q d_{u-i-v,j}^0 \\
& \binom{u}{i} \binom{u}{n+i} c_{l,u}^q d_{n+i,i}^q d_{u-n-i,j}^0 - \sum_{n=0}^{u-(i+j)} \binom{q+u}{q+n+i} \binom{u}{n+i} c_{l,u}^q d_{n+i,i}^q d_{u-n-i,j}^0
\end{aligned}$$

By combining (A25), (A29) and (A31), we deduce $SI(q+2l, q)^{(t)} = CL(q+2l, q)^{(t)}$. By Lemma 3, $CL(q+2l, q)^{(t)}$ is invariant to image scaling and rotation, thus, $SI(q+2l, q)^{(t)}$ is also invariant to image scaling and rotation.

The proof has been completed.

Appendix B (List of Zernike Moment Blur Invariants up to the Sixth Order)

- Zero order

$$I(0,0) = Z_{0,0}$$

- First order

$$I(1,1) = Z_{1,1}$$

- Second order

$$I(2,2) = Z_{2,2}$$

- Third order

$$I(3,1) = Z_{3,1} - 6I(1,1) - 2I(1,1)Z_{2,0} / Z_{0,0}$$

$$I(3,3) = Z_{3,3}$$

- Fourth order

$$I(4,2) = Z_{4,2} - 10I(2,2) - 10I(2,2)Z_{2,0} / (3Z_{0,0})$$

$$I(4,4) = Z_{4,4}$$

- Fifth order

$$I(5,1) = Z_{5,1} - 54I(1,1) - 15I(3,1) - [23I(1,1)Z_{2,0} + 3I(1,1)Z_{4,0} + 5I(3,1)Z_{2,0}] / Z_{0,0}$$

$$I(5,3) = Z_{5,3} - 15I(3,3) - 5I(3,3)Z_{2,0} / Z_{0,0}$$

$$I(5,5) = Z_{5,5}$$

- Sixth order

$$I(6,2) = Z_{6,2} - 105I(2,2) - 21I(4,2) - [140I(2,2)Z_{2,0} / 3 + 7I(2,2)Z_{4,0} + 7I(4,2)Z_{2,0}] / Z_{0,0}$$

$$I(6,4) = Z_{6,4} - 21I(4,4) - 7I(4,4)Z_{2,0} / Z_{0,0}$$

$$I(6,6) = Z_{6,6}$$

Appendix C (List of Zernike Moment Combined Invariants up to the Sixth Order)

- Second order

$$SI(2,0) = -3\Gamma_f^{-2}I(0,0) + 3\Gamma_f^{-4}I(0,0) + \Gamma_f^{-4}I(2,0)$$

$$SI(2,2) = e^{-2j\theta_r} \Gamma_f^{-4}I(2,2)$$

- Third order

$$SI(3,1) = e^{-j\theta_r} \Gamma_f^{-5}I(3,1)$$

$$SI(3,3) = e^{-3j\theta_r} \Gamma_f^{-5}I(3,3)$$

- Fourth order

$$SI(4,0) = 5\Gamma_f^{-2}I(0,0) - 15\Gamma_f^{-4}I(0,0) + 10\Gamma_f^{-6}I(0,0) - 5\Gamma_f^{-4}I(2,0) + 5\Gamma_f^{-6}I(2,0) + \Gamma_f^{-6}I(4,0)$$

$$SI(4,2) = e^{-2j\theta_r} [-5\Gamma_f^{-4}I(2,2) + 5\Gamma_f^{-6}I(2,2) + \Gamma_f^{-6}I(4,2)]$$

$$SI(4,4) = e^{-4j\theta_r} \Gamma_f^{-6}I(4,4)$$

- Fifth order

$$SI(5,1) = e^{-j\theta_r} [-6\Gamma_f^{-5}I(3,1) + 6\Gamma_f^{-7}I(3,1) + \Gamma_f^{-7}I(5,1)]$$

$$SI(5,3) = e^{-3j\theta_r} [-6\Gamma_f^{-5}I(3,3) + 6\Gamma_f^{-7}I(3,3) + \Gamma_f^{-7}I(5,3)]$$

$$SI(5,5) = e^{-5j\theta_r} \Gamma_f^{-7}I(5,5)$$

- Sixth order

$$(0, 0) + 42\Gamma_f^{-4}I(0, 0) - 70\Gamma_f^{-6}I(0, 0) + 35\Gamma_f^{-8}I(0, 0) + 14\Gamma_f^{-6}I(2, 0) - 35\Gamma_f^{-6}I(2, 0) + 21\Gamma_f^{-8}I(2, 0) - 7\Gamma_f^{-6}I(4, 0) + 7\Gamma_f^{-4}I(2, 2) - 35\Gamma_f^{-6}I(2, 2) + 21\Gamma_f^{-8}I(2, 2) - 7\Gamma_f^{-6}I(4, 2) + 7\Gamma_f^{-8}I(4, 2) + \Gamma_f^{-8}I(6, 2)] \\ 7\Gamma_f^{-6}I(4, 4) + 7\Gamma_f^{-8}I(4, 4) + \Gamma_f^{-8}I(6, 4)] \\ {}^3I(6, 6)$$

References:

1. Hu MK . Visual pattern recognition by moment invariants . IRE Trans Inform Theory . IT-8 : (2) 179 - 187 1962 ;
2. Reiss TH . The revised fundamental theorem of moment invariants . IEEE Trans Pattern Anal Mach Intell . 13 : (8) 830 - 834 1991 ;
3. Flusser J , Suk T . Pattern recognition by affine moment invariants . Pattern Recognit . 26 : (1) 167 - 174 1993 ;
4. Reddi SS . Radial and angular moment invariants for image identification . IEEE Trans Pattern Anal Machine Intell . 3 : (2) 240 - 242 1981 ;
5. Abu-Mostafa YS , Psaltis D . Recognitive aspects of moment invariants . IEEE Trans Pattern Anal Machine Intell . 6 : (6) 698 - 706 1984 ;
6. Arbter K , Snyder WE , Burkhardt H , Hirzinger G . Application of affine-invariant Fourier descriptors to recognition of 3-D objects . IEEE Trans Pattern Anal Machine Intell . 12 : (7) 640 - 647 1990 ;
7. Suk T , Flusser J . Vertex-based features for recognition of projectively deformed polygons . Pattern Recognit . 29 : (3) 361 - 367 1996 ;
8. Lenz R , Mer P . Point configuration invariants under simultaneous projective and permutation transformations . Pattern Recognit . 27 : (11) 1523 - 1532 1994 ;
9. Rao NSV , Wu W , Glover CW . Algorithms for recognizing planar polygonal configurations using perspective images . IEEE Trans Robotics Automat . 8 : (4) 480 - 486 1992 ;
10. Lowe DG . Distinctive image features from scale-invariant key points . Int J Computer Vision . 60 : (2) 91 - 110 2004 ;
11. Khotanzad A , Hong YH . Invariant image recognition by Zernike moments . IEEE Trans Pattern Anal Machine Intell . 12 : (5) 489 - 497 1990 ;
12. Zhang F , Liu SQ , Wang DB , Guan W . Aircraft recognition in infrared image using wavelet moment invariants . Image Vision Computing . 27 : (4) 313 - 318 2008 ;
13. Yang CY , Chou JJ . Classification of rotifers with machine vision by shape moment invariants . Aquac Eng . 24 : (1) 33 - 57 2000 ;
14. Lin YH , Chen CH . Template matching using the parametric template vector with translation, rotation and scale invariance . Pattern Recognit . 41 : (7) 2413 - 2421 2008 ;
15. Flusser J , Suk T , Saic S . Recognition of blurred images by the method of moments . IEEE Trans Image Process . 5 : (3) 533 - 538 1996 ;
16. Savakis A , Trussell HJ . Blur identification by residual spectral matching . IEEE Trans Image Process . 2 : (2) 141 - 151 1993 ;
17. Banham MR , Katsaggelos AK . Digital image restoration . IEEE Signal Process Mag . 14 : (2) 24 - 41 1997 ;
18. Molina R , Mateos J , Katsaggelos AK . Blind deconvolution using a variational approach to parameter, image, and blur estimation . IEEE Trans Image Process . 15 : (12) 3715 - 3727 2006 ;
19. Sorel M , Flusser J . Space-variant restoration of images degraded by camera motion blur . IEEE Trans Image Process . 17 : (2) 105 - 116 2008 ;
20. Ojansivu V , Heikkila J . A method for blur and affine invariant object recognition using phase-only bispectrum . Springer ; ICIAR, LNCS 5112 . 527 - 536 2008 ;
21. Jung SW , Kim TH , Ko SJ . A novel multiple image deblurring technique using fuzzy projection onto convex sets . IEEE Signal Process Lett . 16 : (3) 192 - 195 2009 ;
22. Flusser J , Suk T . Degraded image analysis: an invariant approach . IEEE Trans Pattern Anal Machine Intell . 20 : (6) 590 - 603 1998 ;
23. Liu J , Zhang TX . Recognition of the blurred image by complex moment invariants . Pattern Recognit Lett . 26 : (8) 1128 - 1138 2005 ;
24. Flusser J , Suk T , Saic S . Recognition of images degraded by linear motion blur without restoration . Comput Suppl . 11 : 37 - 51 1996 ;
25. Stern A , Kruchakov I , Yoavi E , Kopeika S . Recognition of motion-blurred images by use of the method of moments . Appl Opt . 41 : (11) 2164 - 2172 2002 ;
26. Lu J , Yoshida Y . Blurred image recognition based on phase invariants . IEICE Trans Fundam Electron Comm Comput Sci . E82A : 1450 - 1455 1999 ;
27. Wang XH , Zhao RC . Pattern recognition by combined invariants . Chin J Electron . 10 : (4) 480 - 483 2001 ;
28. Nentoutou Y , Taleb N , Mezour M , Taleb M , Jetto L . An invariant approach for image registration in digital subtraction angiography . Pattern Recognit . 35 : (12) 2853 - 2865 2002 ;
29. Zhang Y , Zhang Y , Wen C . A new focus measure method using moments . Image Vision Computing . 18 : (12) 959 - 965 2000 ;
30. Flusser J , Suk T , Saic S . Image feature invariant with respect to blur . Pattern Recognit . 28 : (11) 1723 - 1732 1995 ;
31. Flusser J , Suk T , Saic S . Recognition of images degraded by linear motion blur without restoration . Comput Suppl . 11 : (1) 37 - 51 1996 ;
32. Stern A , Kruchakov I , Yoavi E , Kopeika S . Recognition of motion-blurred image by use of the method of moments . Appl Opt . 41 : 2164 - 2172 2002 ;
33. Flusser J , Zitova B . Combined invariants to linear filtering and rotation . Int J Pattern Recognit Artif Intell . 13 : (8) 1123 - 1136 1999 ;
34. Flusser J , Zitova B , Suk T . Invariant-based registration of rotated and blurred images . Editor: Tammy IS . Proc. of the IEEE International Geoscience and Remote Sensing Symposium IGARSS'99, Hamburg, Germany 1262 - 1264 June 1999
35. Zitova B , Flusser J . Estimation of camera planar motion from defocused images . Proc. of the IEEE International Conference on Image Processing ICIP'02, II : Rochester, NY 329 - 332 September, 2002.
36. Zhang Y , Wen C , Zhang Y , Soh YC . Determination of blur and affine combined invariants by normalization . Pattern Recognit . 35 : (1) 211 - 221 2002 ;
37. Suk T , Flusser J . Combined blur and affine moment invariants and their use in pattern recognition . Pattern Recognit . 36 : (12) 2895 - 2907 2003 ;
38. Flusser J , Boldys J , Zitova B . Moment forms invariant to rotation and blur in arbitrary number of dimensions . IEEE Trans Pattern Anal Machine Intell . 25 : (2) 234 - 246 2003 ;
39. Candocia FM . Moment relations and blur invariant conditions for finite-extent signals in one, two and N-dimensions . Pattern Recognit Lett . 25 : (4) 437 - 447 2004 ;
40. Zhang H , Shu HZ , Han GN , Coatrieux G , Luo LM , Coatrieux JL . Blurred image recognition by Legendre moment invariants . IEEE Trans Image Process . 19 : (3) 596 - 611 2010 ;
41. Liu HQ , Liu M , Ji HJ , Li Y . Combined invariants to blur and rotation using Zernike moment descriptors . Pattern Anal Applic . 10.1007/s10044-009-0159-9 2009 ;
42. Ji H , Zhu H . Degraded image analysis using Zernike moments . Proc. of 2009 IEEE International Conference on Acoustics, Speech and Signal Processing, ICASSP 2009, Taipei, Taiwan 1941 - 1944 Apr. 19-24, 2009.
43. Flusser J , Zitova B . Invariants to convolution with circularly symmetric PSF . Proc. of the 17th International Conference on Pattern Recognition, ICPR'04, Cambridge, UK 2 : 11 - 14 2004 ;
44. Mukundan R , Ramakrishnan KR . Moment Functions in Image Analysis—Theory and Applications . World Scientific ; Singapore 1998 ;
45. Shu HZ , Luo LM , Han GN , Coatrieux JL . A general method to derive the relationship between two sets of Zernike coefficients corresponding to different aperture sizes . J Opt Soc Am A . 23 : (8) 1960 - 1966 2006 ;
46. Flusser J . On the independence of rotation moment invariants . Pattern Recognit . 33 : (9) 1405 - 1410 2000 ;
47. <http://www.cs.umb.edu/~whaber/Monte/BF/Ithomid-spec.html> .
48. Xin Y , Pawlak M , Liao S . Accurate computation of Zernike moments in polar coordinates . IEEE Trans Image Process . 16 : (2) 581 - 587 2007 ;
49. Liao SX , Pawlak M . On image analysis by moments . IEEE Trans Pattern Anal Machine Intell . 18 : (3) 254 - 266 1996 ;
50. Teh CH , Chin RT . On image analysis by the method of moments . IEEE Trans Pattern Anal Machine Intell . 10 : (4) 496 - 513 1988 ;
51. Lindeberg T . Feature detection with automatic scale selection . International Journal of Computer Vision . 30 : (2) 79 - 116 1998 ;

Fig. 1

Eighteen objects selected from a butterfly database

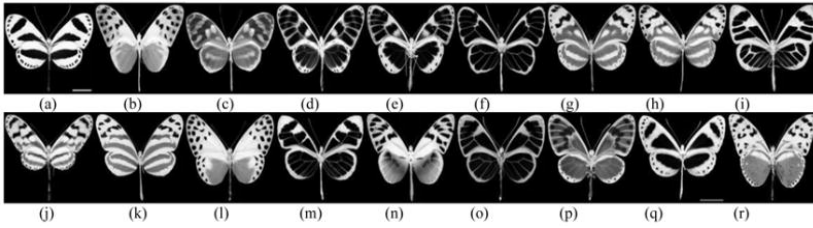


Fig. 2

The mean relative errors of our combined invariants ZMIs for different rotated and blurred versions of the images shown in Fig. 1 .

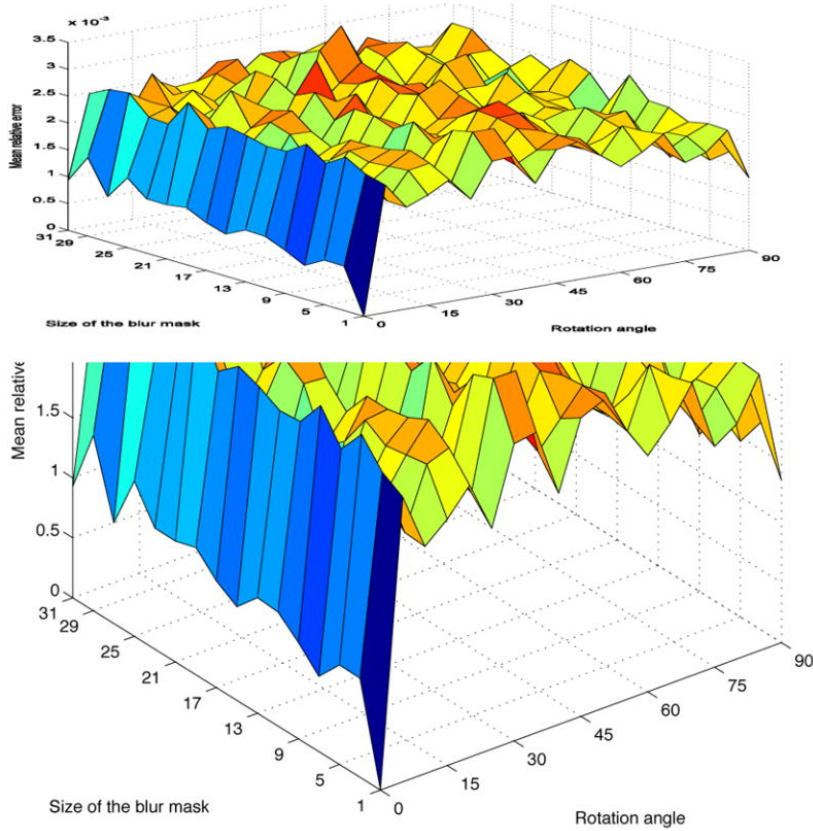


Fig. 3

The mean relative errors of our combined invariants ZMIs for different scaled and blurred versions of the images shown in Fig. 1 .

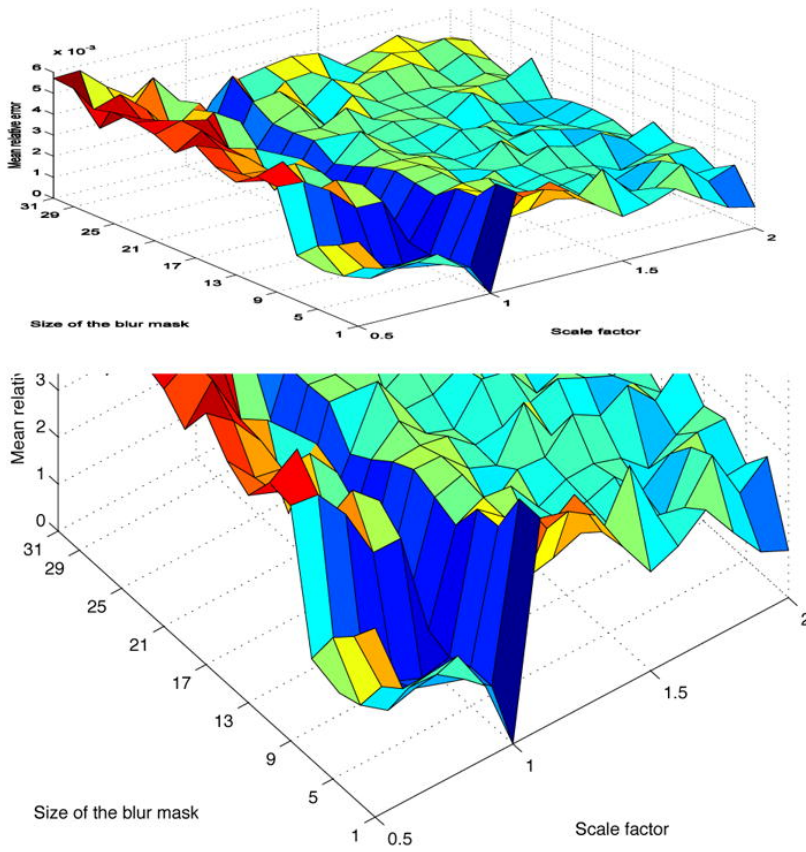


Fig. 4

The similarity transformed and blurred images of Fig. 1(a) (Δx is the translation (in pixel) along the x-axis, Δy the translation along the y-axis, λ the scaling factor, θ the rotation angle, $k \times k$ is the mask size)

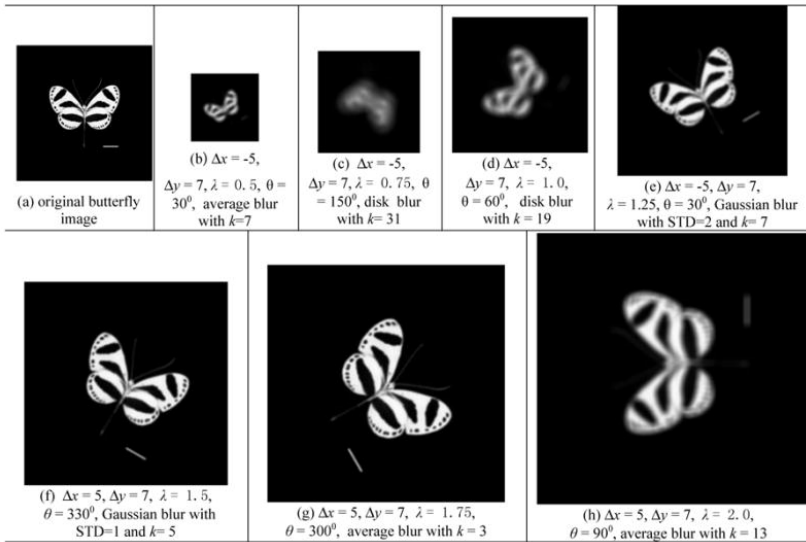


Fig. 5

The mean relative errors of CMIs, LMIs and ZMIs for different blurred versions of the images shown in Fig. 1 .

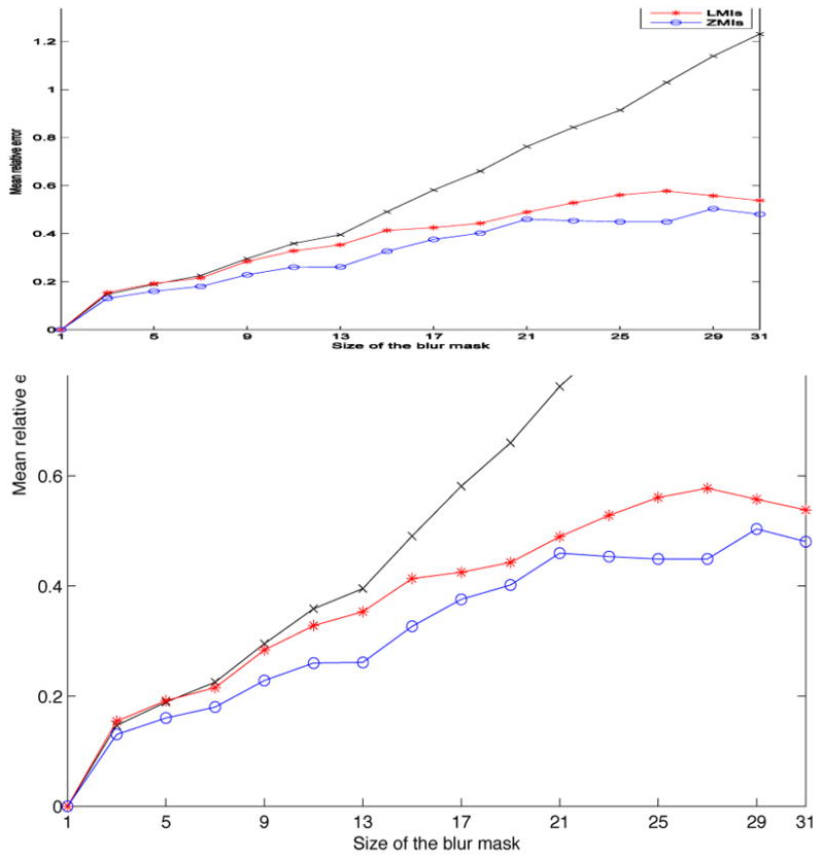


Fig. 6

Examples of image with different blur, different mask sizes and different noises (δ is the STD of Gaussian noise, p is the density of salt-and-pepper noise)

	average blur with mask size 15×15	disk blur with mask size 11×11	disk blur with mask size 19×19	Gaussian blur with STD=1 and mask size 9×9	Gaussian blur with STD=2 and mask size 19×19
Noise-free					
Gaussian noise					
Salt-and-pepper noise					

Fig. 7

The mean classification rates (%) of the LMIs, CMIs and the proposed ZMIs in object recognition for different moment orders

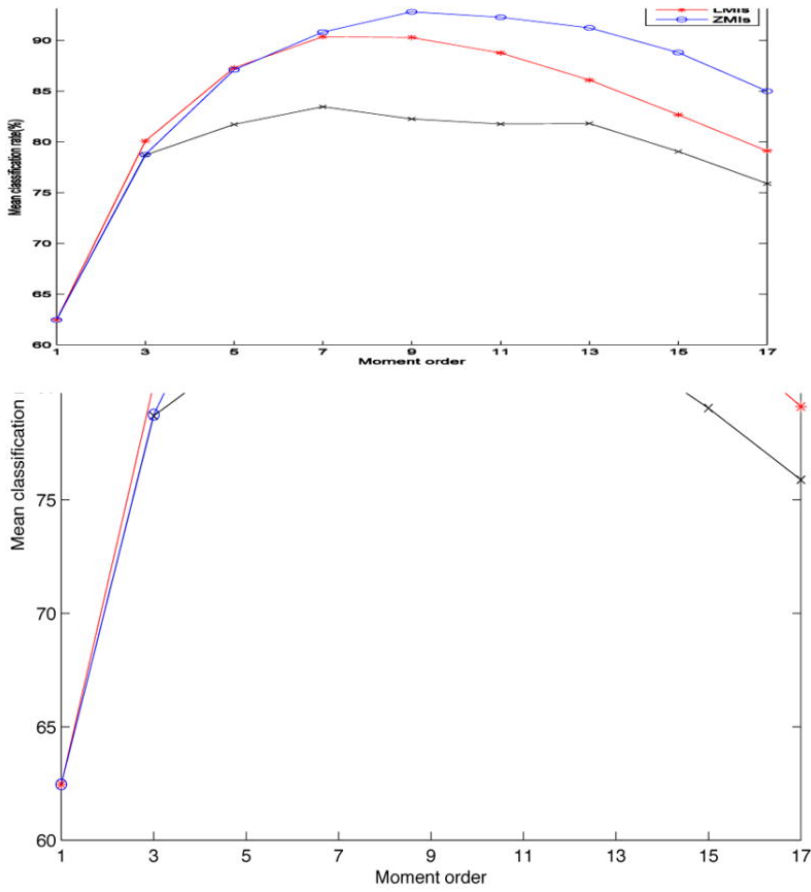


Fig. 8

Images of the outdoor scene. (a) The original image, (b) The transformed and blurred image, (c) The matched templates using CMIs, (d) The matched templates using the proposed ZMIs

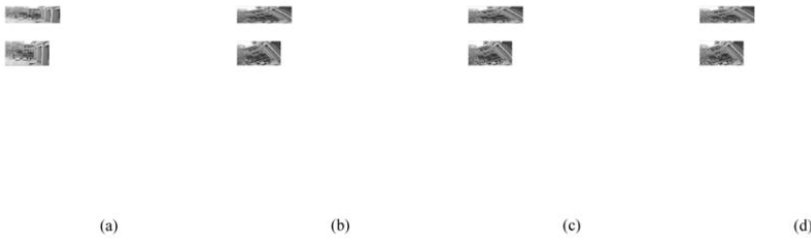


Table 1

The invariants of images showed in Fig. 4

	Fig. 4(a)	Fig. 4(b)	Fig. 4(c)	Fig. 4(d)	Fig. 4(e)	Fig. 4(f)	Fig. 4(g)	Fig. 4(h)
SI (2,2)	6.95e-03	6.95e-03	6.97e-03	6.96e-03	6.95e-03	6.94e-03	6.95e-03	6.95e-03
SI (3,1)	2.72e-04	2.70e-04	2.76e-04	2.73e-04	2.71e-04	2.72e-04	2.71e-04	2.71e-04
SI (3,3)	5.87e-04	5.88e-04	5.90e-04	5.88e-04	5.87e-04	5.88e-04	5.87e-04	5.87e-04
SI (4,2)	3.51e-02	3.51e-02	3.52e-02	3.51e-02	3.51e-02	3.51e-02	3.51e-02	3.51e-02
SI (4,4)	3.58e-05	3.59e-05	3.49e-05	3.56e-05	3.57e-05	3.58e-05	3.58e-05	3.58e-05
SI (5,1)	1.66e-03	1.65e-03	1.69e-03	1.67e-03	1.66e-03	1.66e-03	1.66e-03	1.66e-03
SI (5,3)	3.57e-03	3.57e-03	3.58e-03	3.57e-03	3.56e-03	3.57e-03	3.56e-03	3.57e-03
SI (5,5)	9.92e-06	9.96e-06	9.93e-06	9.93e-06	9.93e-06	9.92e-06	9.92e-06	9.92e-06

Table 2

The classification rates (%) of the LMIs, CMIs and the proposed ZMIs in object recognition with the optimal value of M

	CMIs	LMIs	ZMIs
Noise-free	98.77	99.07	99.85
Gaussian noise with STD = 16	97.38	97.84	98.92
Gaussian noise with STD = 25	93.83	96.91	97.84
Gaussian noise with STD = 36	81.48	92.44	94.60
Gaussian noise with STD = 49	63.12	81.64	85.80
Gaussian noise with STD = 64	48.30	66.98	76.08
Salt-and-pepper noise with noise density = 1%	97.84	98.61	99.69
Salt-and-pepper noise with noise density = 3%	96.45	96.91	97.84
Salt-and-pepper noise with noise density = 5%	87.04	93.52	94.60
Salt-and-pepper noise with noise density = 7%	81.02	88.58	91.05
Salt-and-pepper noise with noise density = 9%	72.69	82.10	84.57
Mean rate	83.45	90.42	92.80